Integrated analysis of the transcriptome-wide m6A methylome in preeclampsia and healthy control placentas

Jin Wang [1], **Yan Cai** [1], **Fengchun Gao** [2], **Xiaohan Zhao** [1], **Hua Jin** [Corresp. 1]

[1] Prenatal Diagnosis Center, Jinan Maternal and Child Health Care Hospital, Jinan, China

[2] Obstetrical Department, Jinan Maternal and Child Health Care Hospital, Jinan, China

Corresponding Author: Hua Jin
Email address: wangjinshiyi@126.com

N6-methyladenosine (m6A) is the most prevalent modification in eukaryotic mRNA and potential regulatory functions of m6A have been shown by mapping the RNA m6A modification landscape. M6A modification in active gene regulation manifests itself as altered methylation profiles. However, the profiling of m6A modification and its potential role in preeclampsia (PE) has not yet been studied. In this work, placental samples were collected from PE and control patients. Expression of m6A-related genes was investigated using quantitative real-time PCR. MeRIP-seq and RNA-seq were performed to detect m6A methylation and mRNA expression profiles. Gene ontology (GO) functional and Kyoto encyclopedia of genes and genomes (KEGG) pathway analyses were also conducted to explore the modified genes and their clinical significance. Our findings show that METTL3 and METTL14 were up-regulated in PE. In total, 685 m6A peaks were differentially expressed as determined by MeRIP-seq. Altered peaks of m6A-modified transcripts were primarily associated with nitrogen compound metabolic process, positive regulation of vascular-associated smooth muscle cell migration, and endoplasmic reticulum organisation. The m6A hyper-methylated genes of Wnt/β-catenin signalling pathway, mTOR signalling pathway, and several cancer-related pathways may contribute to PE. We also found a relationship between the extent of m6A and the level of transcript, suggesting m6A plays a key role in the regulation of gene expression. Our data provide novel information regarding m6A modification alterations in PE and help our understanding of the pathogenesis of PE.

Integrated analysis of the transcriptome-wide m6A methylome in preeclampsia and healthy control placentas

Jin Wang[1], Yan Cai[1], Fengchun Gao[2], Xiaohan Zhao[1], Hua Jin[*,1]

[1]Prenatal Diagnosis Center, Jinan Maternal and Child Health Care Hospital, Jinan, Shandong Province, PR China

[2]Obstetrical Department, Jinan Maternal and Child Health Care Hospital, Jinan, Shandong Province, PR China

* Corresponding Author:

Hua Jin

No.2, Jianguo xiaojing roud, Jinan 250002, Shandong Province, PR China

Email address: wangjinshiyi@126.com

Abstract

N6-methyladenosine (m6A) is the most prevalent modification in eukaryotic mRNA and potential regulatory functions of m6A have been shown by mapping the RNA m6A modification landscape. M6A modification in active gene regulation manifests itself as altered methylation profiles. However, the profiling of m6A modification and its potential role in preeclampsia (PE) has not yet been studied. In this work, placental samples were collected from PE and control patients. Expression of m6A-related genes was investigated using quantitative real-time PCR. MeRIP-seq and RNA-seq were performed to detect m6A methylation and mRNA expression profiles. Gene ontology (GO) functional and Kyoto encyclopedia of genes and genomes (KEGG) pathway analyses were also conducted to explore the modified genes and their clinical significance. Our findings show that METTL3 and METTL14 were up-regulated in PE. In total, 685 m6A peaks were differentially expressed as determined by MeRIP-seq. Altered peaks of m6A-modified transcripts were primarily associated with nitrogen compound metabolic process, positive regulation of vascular-associated smooth muscle cell migration, and endoplasmic reticulum organisation. The m6A hyper-methylated genes of Wnt/β-catenin signalling pathway, mTOR signalling pathway, and several cancer-related pathways may contribute to PE. We also found a relationship between the extent of m6A and the level of transcript, suggesting m6A plays a key role in the regulation of gene expression. Our data provide novel information regarding m6A modification alterations in PE and help our understanding of the pathogenesis of PE.

Introduction

Preeclampsia (PE) is a multi-system disorder that is primarily characterised by new-onset hypertension accompanied by proteinuria during gestation. This disease affects 3–5% of all pregnancies and is one of the leading causes of maternal and perinatal morbidity and mortality (Mol et al. 2016). The exact pathophysiology that causes PE remains unclear; however, genetic, immunological, endocrine, and environmental factors have been implicated in its pathogenesis (Burton et al. 2019). The placenta plays an essential role in the development of PE. The underlying pathogenic mechanisms include defective deep placentation, oxidative and endoplasmic reticulum stress, intravascular inflammation, and imbalance of angiogenesis, among others (Burton et al. 2019; Chaiworapongsa et al. 2014). No specific treatment is currently available, and delivery of the placenta is the only effective treatment (Burton et al. 2019; Chaiworapongsa et al. 2014; Wang et al. 2019).

Numerous studies have reported that PE significantly alters the expression of coding and noncoding RNAs (ncRNAs), including mRNA, miRNA, long noncoding RNA (lncRNA), and circular RNA (circRNA) (Bai et al. 2018; Liu et al. 2017b; Muller-Deile et al. 2018; Nikuei et al. 2017). However, while these studies explored RNA expression, the modification profiles of these RNAs in the context of PE remain to be characterised. N6-methyladenosine (m6A) modification in mRNA is prevalent, and functionally modulates in eukaryotes that is mediated by the m6A methyltransferase complex, methyltransferase-like (METTL)3, METTL14, and Wilms' tumour 1-associated protein

(WTAP) and eliminated by fat-mass and obesity-associated protein (FTO) or alkylation repair homolog protein 5 (ALKBH5) (Boccaletto et al. 2018; Fu et al. 2014; Meyer & Jaffrey 2014). These modifications are believed to moderate RNA structure, function, and stability (Edupuganti et al. 2017; Liu et al. 2017a; Piao et al. 2017; Wang et al. 2014). Recently, the effects of m6A modification on many fundamental biological processes have been characterised; these processes include metabolism (Yang et al. 2018), immunomodulation (Zheng et al. 2017), carcinogenesis(Ma et al. 2017; Zhang et al. 2017a), and spermatogenesis (Chen et al. 2017), among others. Abnormal m6A methylation is associated with a variety of human diseases, such as obesity, neuronal disorders, cancer, and infertility (Chen et al. 2017; Ma et al. 2017; Yang et al. 2018; Zhang et al. 2017a; Zheng et al. 2017).

Given the indispensable function of RNA m6A modification in various bioprocesses, it is reasonable to speculate that deregulation of m6A modification may also be associated with PE. A recent study indicate that m6A at 5'-UTR and nearby stop codon in placental mRNA may play important roles in fetal growth and PE through conducted MeRIP-Seq on human placentas obtained from mothers of infants of various birth weights (Taniguchi et al. 2020). Here, we aimed to compare the m6A-tagged transcript profiles of placentas from PE-affected pregnancies with those of placentas from healthy pregnancies to identify gene-specific changes in RNA methylation that may regulate placental gene expression and contribute to the development of PE. Additionally, potential roles for the m6A-modified transcripts in the physiological and pathological

mechanisms underlying PE were revealed; these can provide a theoretical basis for the prevention and pre-emptive treatment of PE.

Materials & Methods

Sample collection

All placental samples used in this study were collected from the Department of Obstetrics, Jinan Maternal and Child Health Care Hospital. The characteristics of puerperants and newborns were collected from hospital medical records. PE cases (n =4) were collected in light of the guideline designed by the American College of Obstetrics and Gynecology (ACOG) (2019; Magee et al. 2014). These cases included women who exhibited a blood pressure of ≥140/90 mmHg on two occasions that occurred at least 4 h apart, accompanied by proteinuria (2+ on dipstick or 300 mg/24 h) at ≥20 weeks and <34 weeks of gestation. Normal controls (n =4) were defined as pregnancies without PE. All participants were of Han Chinese descent and those with complications such as gestational hypertension, gestational diabetes mellitus, foetal growth restriction, or preterm birth (<37 weeks) were excluded (Table 1). The study protocols were approved by the Ethics Review Committee of Ji'nan Maternal and Child Health Care Hospital and conducted in accordance with the Declaration of Helsinki (No. JNFY-2019003).

Placental samples were collected at three sites from the foetal side of the placenta immediately after caesarean section (<30 min). Fragments of approximately 1 cm^3 were dissected from the placenta after removing maternal blood by vigorous washing in ice-cold saline; these fragments were snap-frozen in liquid nitrogen and stored at -80°C until

use. All participants provided written informed consent prior to participation.

RNA isolation

The placental samples from three different sites were ground and mixed, then, total RNA was isolated using TRIzol reagent (Invitrogen, CA, USA) according to the manufacturer's protocol. Agarose gel electrophoresis and NanoDrop ND-1000 (Thermo Fisher Scientific, MA, USA) was used to monitor RNA integrity and quality. Intact mRNA was isolated from the total RNA samples using an Arraystar Seq-Star™ poly(A) Mrna Isolation Kit in accordance with the manufacturer's protocol.

Quantitative real-time PCR

The expression of m6A-related genes *METTL3*, *METTL14*, *FTO*, *WTAP*, and *ALKBH5* were detected by quantitative real-time PCR (qPCR). Briefly, total RNA was isolated using TRIzol reagent (Invitrogen), and cDNA was generated by reverse transcription using Prime Script™ RT Master Mix (Perfect Real-Time; Takara Bio, Shiga, Japan). Quantitative real-time PCR (RT-PCR) was performed using SYBR Green master mix (Yeasen, Shanghai, China) and a thermal cycler (LightCycler System; Roche Diagnostics Corp, IN, USA). β-Actin was used as an internal control to normalise the data. The primers used for RT-qPCR are presented in Table 2.

Quantification of m6A in total RNA.

Total RNA was isolated from the placental tissue using TRIzol according to the manufacturer's instructions. RNA was tested for quality using a Nanodrop ND-1000 (Thermo Fisher Scientific, MA, USA) and gel electrophoresis. The M6A RNA methylation

121 status was directly detected using the EpiQuik™ m6A RNA Methylation Quantification
122 Kit (Colorimetric) according to the manufacturer's protocol. Briefly, a negative control and
123 a standard curve consisting of six different concentrations (range: from 0.02 to 1 ng of
124 m6A) were prepared. Two hundred nanograms of total RNA was used for each reaction.
125 After RNA binding to the 96-well plates, the binding solution was removed and the plates
126 were washed three times with diluted wash buffer. Then, diluted capture anti-m6A
127 antibodies were added; subsequently, the plates were washed four times with diluted
128 wash buffer. Add 100 μl of developer solution to each well and incubate at room
129 temperature for 7 min away from light. Add 100 ul of stop solution to each well to stop
130 enzyme reaction. The optical density (OD) at 450 nm was measured using a microplate
131 reader (BIOTEK, Vermont, USA). The absolute amount of m6A was quantified, and the
132 percentage of m6A within the total RNA was calculated.

133 **M6A-RIP-seq and data analysis**

134 Poly(A) RNA was extracted with Arraystar Seq-Star^{TM} poly(A) mRNA Isolation Kit
135 (Arraystar, MD, USA). The RNA was fragmented into fragments with an average length
136 of 100 nt using RNA Fragmentation Reagents (Sigma, MO, USA). Fragmented mRNAs
137 were incubated for 2 h at 4 °C in the presence of 2 μg m6A antibodies (Synaptic Systems,
138 202003) in a 500 μl IP reaction system, and some of the fragments were used as input.
139 The mixture was then incubated with protein-A beads and purified using elution buffer
140 and ethanol. RNA-seq libraries for m6A antibody-enriched mRNAs and input mRNAs
141 were prepared using the KAPA Stranded mRNA-seq Kit (Illumina, CA, USA). Finally, the

completed libraries were assessed using an Agilent 2100 Bioanalyzer. The libraries were denatured with 0.1M NaOH and loaded into the reagent cartridge. Clusters were generated using an Illumina cBot system (#PE-410-1001, Illumina). Sequencing was performed on an Illumina HiSeq 4000 machine following HiSeq 3000/4000 SBS Kit (300 cycles) protocols.Quality control of the sequence data was performed using FastQC (v0.11.7). The raw data were trimmed using Trimmomatic software (v0.32) and aligned to the Ensembl reference genome using HISAT2 software (v2.1.0). The m6a-RIP-enriched regions (peaks) were detected using exomePeak software (v2.13.2). The differential m6A peaks (fold changes ≥1.5 and $p < 0.05$) between the case group and control group were analysed using exomePeak. These differential peaks were annotated using the Ensembl database (GRCh 37/hg19). DREME motif discovery in transcription factor ChIP-seq data was used to identify motifs among the m6A peak sequences. Gene ontology (GO) terms and Kyoto encyclopedia of genes and genomes (KEGG) pathways were analyzed through GO database and KEGG pathway database.

RNA-Sequencing

Total RNA was isolated from the placental tissue using TRIzol reagent (Invitrogen), and the quality and quantity of RNA were assessed by NanoDrop and gel electrophoresis. Intact mRNA was isolated from total RNA samples using a NEBNext Poly(A) mRNA Magnetic Isolation Module (New England Biolabs, Hertfordshire, UK) according to the manufacturer's protocol. RNA-Seq libraries were prepared using a KAPA Stranded RNA-Seq Library Prep Kit (Illumina). Sequencing was performed using the Illumina HiSeq

4000 platform.

Statistical analyses

Data are expressed as the mean ± standard deviation (SD). All statistical analyses were conducted using the SPSS 22.0 statistical package. Student's t-test was used to compare the fluorescence intensity of the m6A-related genes (METTL3, METTL14, FTO, WTAP, and ALKBH5) between the PE and control samples. Fisher's exact test was used for all bioinformatic analyses, and a p-value < 0.05 was considered statistically significant.

Results

The main clinical information of samples

The main clinical data of the PE cases and controls are summarised in Table 1. All women did not have diabetes, chronic hypertension, polycystic ovarian syndrome, kidney or liver disease, and serious infection. Blood pressure and proteinuria were significantly higher in the PE cases than in the controls. There was no significant difference in maternal age, gestational age, prenatal maternal body mass index, and birth weights at delivery between the groups.

METTL3 and METTL14 were up-regulated in PE

Using qRT-PCR, we examined the mRNA levels of five core enzymes responsible for m6A modification, including METTL3, METTL14, FTO, WTAP, and ALKBH5, in the PE and control samples. mRNA levels of METTL3 and METTL14, the key m6A methyltransferase, were significantly increased in the PE samples compared to the

control (Fig. 1; METTL3 $p = 0.023$; METTL14 $p = 0.016$). WTAP and the erasers FTO and ALKBH5 were not significantly dysregulated in the PE group (Fig. 1).

M6A modification profiles in PE

In this study, each sample was generated nearly 20 M m6A-RIP-seq reads, and the quality control metrics of the sequence data are shown in Table S1. The level of m6A RNA methylation within the total RNA in the PE was higher than that in the controls (Fig. 2). We then analysed the genome-wide profiling of the m6A-modified mRNA in the PE and control samples (GEO accession number: GSE143966). In total, 370 m6A peaks were significantly up-regulated, whereas 315 peaks were down-regulated (fold changes ≥1.5 and $p < 0.05$; Fig. 3A). The top 20 altered methylated m6A peaks are listed in Table 3, and all significantly differentially expressed m6A peaks are listed in Table S2. The identified m6A peaks were primarily enriched within the coding sequence in proximity to the stop codons and in the 3′UTR (Fig. 3B & C). The distribution patterns of the altered m6A peaks in the placental samples illustrated that the dysregulated m6A peaks could be found in all chromosomes, especially in chr1, chr16, and chr19 (Fig. 3D). Additionally, the m6A peaks were characterised by the canonical RRACH motif (R represents purine, A is m6A, and H is a non-guanine base; Fig. 3E). *HSPA1A*, a representation of the significantly up-regulated peak, is shown in Figure 3F.

GO analysis and pathway analysis of differentially methylated mRNA

To investigate the functional physiological and pathological significance of m6A modification in PE, GO functional analysis and KEGG pathway analysis were used to

examine the altered m6A peaks. GO analysis (the count of genes involved in a GO term > 2, $p < 0.05$) revealed that the up-regulated peaks in PE were significantly involved in macromolecule metabolic processes and the maintenance of DNA repeat elements, nuclear and intracellular processes, and damaged DNA binding and heat shock protein binding (Fig. 4A). The down-regulated peaks were significantly associated with organelle organisation and membrane docking, intracellular and intracellular organelle functions, and damaged DNA binding and cysteine-type endopeptidase activity involved in the execution phase of apoptosis (Fig. 4B).

KEGG pathway analysis demonstrated that the up-regulated peaks in the PE group were significantly associated with the Wnt signalling pathway, the mTOR signalling pathway, and the AMPK signalling pathway (Fig. 4C). The down-regulated peaks were significantly associated with amino sugar and nucleotide sugar metabolism (Fig. 4D).

Overview of transcriptome profiles and conjoint analysis of m6A-RIP-seq and RNA-seq data

In this study, each sample was generated nearly 20 M RNA-seq reads, and the quality control metrics of the RNA-seq data are shown in Table S1. Transcriptome profiles of the altered genes in PE were determined by RNA-seq (GEO accession number: GSE143953). Significantly differentially expressed genes (fold change ≥1.5 and $p < 0.05$) between the PE and control samples were identified using a volcano plot (Fig. 5A); these included 68 up-regulated and 52 down-regulated genes. The top twenty altered genes are listed in Table 4. The top ten GO and pathways associated with the up- or down-

regulated genes are displayed in Supplemental Fig. S1. Hierarchical cluster analysis was performed to identify differentially expressed genes between the two groups (Fig. 5B). The coding potential assessing tool was used to evaluate whether the novel transcripts possessed coding capabilities (Fig. 5C). According to conjoint analysis of m6A-RIP-seq and RNA-seq data, all genes were initially divided into four groups that included 55 hyper-methylated m6A peaks in mRNA transcripts that were significantly up-regulated (30; hyper-up) or down-regulated (25; hyper-down) and 50 hypo-methylated m6A peaks in mRNA transcripts that were significantly up-regulated (34; hypo-up) or down-regulated (16; hypo-down) (Fig. 5D, Table S3).

Discussion

It has long been accepted that placental structural and functional abnormalities can cause a number of pregnancy-associated diseases such as PE, gestational diabetes mellitus, intrauterine growth restriction, and gestational trophoblastic disease (Burton & Jauniaux 2018; Burton et al. 2019; Chaiworapongsa et al. 2014; Mol et al. 2016; Salomon et al. 2016; Veras et al. 2017). Portions of the placenta entering systemic circulation cause maternal PE syndrome, which includes oxidative stress of the syncytiotrophoblast and dysregulated uteroplacental perfusion (Burton et al. 2019; Redman et al. 2014). PE is also associated with changes in placental DNA methylation(Herzog et al. 2017) and gene expression (Junus et al. 2012; Liang et al. 2016). This study was the first to reveal a region-specific m6A methylation map and investigate the role of placental m6A in PE. First, we found that METTL3 and METTL14

were up-regulated in PE as determined by qPCR. Consistent with this result, the total RNA m6A levels were increased in PE. Then, we identified numerous m6A changes in PE placentas compared to healthy controls after excluding the influence of maternal age, body mass index, perinatal complications, and gestational age at diagnosis and delivery. A portion of the genes identified in this study were previously associated with PE ; however, we also identified a number of novel genes. Studies of the human placenta not only enrich our understanding of the mechanisms underlying PE but also provide a theoretical basis for the prevention and pre-emptive treatment of related diseases. Recent studies suggest that the placenta may play a specific role in mediating the generation of intergenerational inheritance (Padmanabhan et al. 2013). Therefore, an in-depth study of the placenta is crucial to determine the mechanisms underlying developmental programming; any related interventions can not only improve maternal and foetal health during pregnancy but also improve the health of multiple generations.

M6A methylation plays a critical role in the regulation of coordinate transcriptional and post-transcriptional gene expression (Edupuganti et al. 2017; Fu et al. 2014; Liu et al. 2017a; Piao et al. 2017; Wang et al. 2014; Yue et al. 2015; Zheng et al. 2017), including mRNA splicing, export, localisation, translation, and stability. M6A within a transcript can facilitate the binding of regulatory proteins and affect the potential of a given transcript for translation. Recent studies have demonstrated a vital functional role for m6A modification in promoting mRNA translation (Shi et al. 2017; Wang et al. 2015). In this study, hundreds of abnormal m6A methylations were also found in the transcripts,

including within zinc finger transcription factors, which uncovers emerging links between m6A mRNA methylation and genome transcription. Thus, RNA decoration by m6A in these transcripts that promotes their interaction with nuclear transcription factors, possibly conferencing recognition of these transcripts (Dominissini et al. 2012).

HSPA1A (heat shock protein 70, Hsp70) is a member of the chaperone machinery that plays a central role in maintaining cellular homeostasis; this protein can elicit innate and adaptive pro-inflammatory immune responses and reflect oxidative stress in PE (Molvarec et al. 2011; Witkin et al. 2017), which is relevant to the progression of PE (Chaiworapongsa et al. 2014). Interestingly, circulating Hsp70 can be directly involved in endothelial activation or injury in PE (Molvarec et al. 2011; Witkin et al. 2017). Indeed, compared with normal pregnancy, Hsp70 was significantly up-regulated in PE placental tissues (Molvarec et al. 2011; Sheikhi et al. 2015; Witkin et al. 2017). However, the exact mechanism of Hsp70 up-regulation in PE remains unclear; it may be related to higher m6A methylation levels of *HSPA1A* in PE placentas than those in the control samples. IGF2BPs are a distinct family of m6A readers that promote the stability and storage of their target mRNAs and therefore affect gene expression output (Huang et al. 2018). Moreover, 92% of the IGF2BP binding sites are located in protein-coding transcripts and highly enriched in CDS near stop codons and in 3'UTRs (Huang et al. 2018). Therefore, we concluded that the increase of m6a methylation in the CDS region of *HSPA1A* may promote mRNA stability. Zhou et al. reported that the m6A modifications of *HSPA1A* were increased at 5'UTR in mouse embryonic fibroblast (MEF) cell line after heat shock

289 stress (Zhou et al. 2015). Compared with this study, the two studies have different
290 species, different tissues, different cells and different treatment process, which may be
291 the reasons for the different results of two studies. Further studies are necessary to
292 elucidate if Hsp70 expression is correlated with m6A methylation of *HSPA1A* in human
293 placenta.

294 GO functional analysis and KEGG pathway analysis identified a possible role for
295 m6A in the pathogenesis of PE. GO analysis identified many “biological processes” that
296 were affected. PE is a multifactorial disease occurring during pregnancy; the underlying
297 pathology is considered to arise from a hypoxic or ischaemic placenta (Burton et al. 2019;
298 Chaiworapongsa et al. 2014; Mol et al. 2016; Myatt & Webster 2009). Peroxynitrite can
299 affect protein activity, function and vascular reactivity in PE, which is the product of the
300 interaction between reactive oxygen species and nitrogen, and mainly comes from
301 placenta and maternal vasculatures (Ahmed et al. 2017; Burton et al. 2019;
302 Chaiworapongsa et al. 2014; Mol et al. 2016; Myatt & Webster 2009; Wu et al. 2016).
303 Interestingly, heightened oxidative/nitrative stress is observed in the maternal
304 vasculature and particularly in the placenta in PE (Myatt & Webster 2009). Here, we offer
305 a new means to explore the role of nitrogen compounds in the pathogenesis of PE. A
306 functional change occurs in the role played by endothelium-derived nitric oxide (NO) in
307 regulating the contraction of resistance arteries and smooth muscles in PE (Pereira et al.
308 2011). Physiological transformation of the uterine spiral arteries is crucial for a
309 successful pregnancy (Burton et al. 2019; Chaiworapongsa et al. 2014; Myatt & Webster

2009; Pereira et al. 2011). This process is closely related to the reduction in the smooth muscle. Conversely, the retention of smooth muscle will increase the risk of ischemia-reperfusion injury, producing oxidative stress, which may lead to shallow placentation and inadequate transformation of the spiral arteries that can lead to PE (Burton et al. 2019; Chaiworapongsa et al. 2014; Myatt & Webster 2009; Pereira et al. 2011). Studies have confirmed that endoplasmic reticulum stress is involved in the regulation of PE (Burton et al. 2019; Chaiworapongsa et al. 2014; Myatt & Webster 2009; Pereira et al. 2011). Endoplasmic reticulum stress is closely related to systemic inflammation and apoptosis, and it regulates the stability in the intracellular environment by participating in post-translational modifications and protein folding (Chaiworapongsa et al. 2014).

KEGG pathway analysis revealed that these target genes were significantly enriched in 20 different pathways, including the “Wnt signalling pathway”, “mTOR signalling pathway”, “AMPK signalling pathway”, and several cancer-related pathways such as “breast cancer”, “basal cell carcinoma”, and “colorectal cancer”, among others. The invasion of extravillous trophoblasts into the uterine wall plays a major role in placental and foetal development, and its dysregulation has been implicated in PE. Mechanistically, trophoblast invasion during embryo implantation strongly resembles the invasion of tumour cells; however, unlike that in tumour cells, this invasion is tightly regulated in both a temporal and spatial manner (Chaiworapongsa et al. 2014; Hiden et al. 2007). Therefore, the normal trophoblast has been termed “pseudo-malignant” (Chaiworapongsa et al. 2014; Hiden et al. 2007). Some of the most essential

331 and crucial pathological changes in the PE process include shallow trophoblast invasion
332 and the damaged spiral artery remodelling, which may be regulated by Wnt/β-catenin
333 signalling pathway (Zhang et al. 2017b). As a canonical Wnt-signalling pathway, the
334 Wnt/β-catenin signalling pathway can regulate several biological processes such as
335 proliferation, migration, invasion, and apoptosis (Nusse & Clevers 2017; Zhang et al.
336 2017b). Abnormal functioning of the Wnt/β-catenin signalling pathway may play an
337 important role in the pathogenesis of various human diseases, including human cancer
338 and PE (Nusse & Clevers 2017; Zhang et al. 2017b); however, direct evidence of the role
339 of the Wnt/β-catenin pathway in the development of PE is lacking. In this study, genes
340 exhibiting abnormal m6A methylation were significantly enriched in the Wnt signalling
341 pathway; this may shed light on a new layer of gene regulation at the RNA level,
342 ultimately giving rise to the field of m6A epitranscriptomics. Interestingly, inhibition of
343 Wnt/β-catenin signalling is a promising treatment approach for a number of cancers
344 (Clara et al. 2019; Krishnamurthy & Kurzrock 2018; Nusse & Clevers 2017). Future
345 studies are recommended to verify if Wnt/β-catenin signalling may provide a prospective
346 therapeutic target for the prevention and treatment of PE.

347 In this study, 120 significantly differentially expressed genes were identified in PE,
348 some genes have been reported in previous studies, including *DIO2*, *BIN2*, *IGSF8*,
349 *BMP5*, and *WNT2* (Sitras et al. 2009; Zhang et al. 2016; Zhang et al. 2017b). These
350 genes, when differentially expressed in different populations, may play an important role
351 in the development of PE. Using bioinformatics analysis, differentially expressed genes

were enriched in biological processes involved in defence response, sphingolipid metabolic processes, and tissue development, among others. Maternal-foetal immune incompatibility and disruption of sphingolipid metabolism have emerged as factors involved in the pathogenic mechanisms underlying PE (Chaiworapongsa et al. 2014; Charkiewicz et al. 2017; Zhang et al. 2017b). This provides further evidence that PE is a heterogeneous and multifactorial disease and that a variety of pathogenic mechanisms are implicated in its occurrence and development.

Conjoint analysis of m6A-RIP-seq and RNA-seq data identified m6A-modified mRNA transcripts that were hyper-methylated or hypo-methylated and significantly differentially expressed. *TCF7L2*, a transcription factor of the Wnt and Hippo signalling pathway, is hyper-methylated and up-regulated in PE, suggesting a possible positive relationship between the extent of m6A methylation and the transcript level. Earlier findings revealed that a *TCF7L2* variant increased the risk of incident hypertension or diabetes mellitus (Bonnet et al. 2013; Chang et al. 2017); however, the relationship between *TCF7L2* and PE is not clear. To provide further insight, it will be necessary, in a future study, to elucidate the biological function of *TCF7L2* in the context of PE.

Gestational age is an important confounder when studying variation in placental DNA methylation. Previous studies have illustrated gestational age as one of the important factors that influence methylation (Novakovic & Saffery 2012; Wilson et al. 2018). Placentas obtained from preterm pregnant women with early PE were used in some studies, to match gestational age, some placentas of women undergoing

spontaneous preterm delivery were used as control groups, which may possess additional differences in methylation that are not detected at full-term (⩾37 week gestation) (Novakovic & Saffery 2012; Wilson et al. 2018; Yeung et al. 2016). In this study, to exclude the influence of gestational age, we used full-term placentas obtained from women with PE; however, we did not perform a study to determine that m6a methylation changes with gestational age. This is a limitation of the present study.

Conclusions

Here, we describe, for the first time, the m6A RNA methylation landscape; reveal the potential functions of this methylation in the regulation of RNA metabolism in PE. Additionally, conjoint analysis of m6A-RIP-seq and RNA-seq data resulted in the identification of differentially expressed hyper-methylated or hypo-methylated mRNA m6A peaks. Further studies will be necessary to validate m6A-enriched genes and examine protein levels of the genes which contribute to elucidate the detailed molecular mechanism underlying the regulation and biological functions of m6A during the PE process. Additionally, characterisation of the role of m6A within the placenta will offer a new viewpoint to elucidate the mechanism of PE.

391 # References

392 2019. ACOG Practice Bulletin No. 202: Gestational Hypertension and Preeclampsia. *Obstet Gynecol* 133:e1-e25.

393 Ahmed A, Rezai H, and Broadway-Stringer S. 2017. Evidence-Based Revised View of the Pathophysiology of
394 Preeclampsia. *Adv Exp Med Biol* 956:355-374.

395 Bai Y, Rao H, Chen W, Luo X, Tong C, and Qi H. 2018. Profiles of circular RNAs in human placenta and their potential
396 roles related to preeclampsia. *Biol Reprod* 98:705-712.

397 Boccaletto P, Machnicka MA, Purta E, Piatkowski P, Baginski B, Wirecki TK, de Crecy-Lagard V, Ross R, Limbach PA,
398 Kotter A, Helm M, and Bujnicki JM. 2018. MODOMICS: a database of RNA modification pathways. 2017
399 update. *Nucleic Acids Res* 46:D303-D307.

400 Bonnet F, Roussel R, Natali A, Cauchi S, Petrie J, Laville M, Yengo L, Froguel P, Lange C, Lantieri O, Marre M, Balkau
401 B, and Ferrannini E. 2013. Parental history of type 2 diabetes, TCF7L2 variant and lower insulin secretion
402 are associated with incident hypertension. Data from the DESIR and RISC cohorts. *Diabetologia* 56:2414-
403 2423.

404 Burton GJ, and Jauniaux E. 2018. Pathophysiology of placental-derived fetal growth restriction. *Am J Obstet*
405 *Gynecol* 218:S745-S761.

406 Burton GJ, Redman CW, Roberts JM, and Moffett A. 2019. Pre-eclampsia: pathophysiology and clinical implications.
407 *BMJ* 366:l2381.

408 Chaiworapongsa T, Chaemsaithong P, Yeo L, and Romero R. 2014. Pre-eclampsia part 1: current understanding of
409 its pathophysiology. *Nat Rev Nephrol* 10:466-480.

410 Chang S, Wang Z, Wu L, Lu X, Shangguan S, Xin Y, Li L, and Wang L. 2017. Association between TCF7L2
411 polymorphisms and gestational diabetes mellitus: A meta-analysis. *J Diabetes Investig* 8:560-570.

412 Charkiewicz K, Goscik J, Blachnio-Zabielska A, Raba G, Sakowicz A, Kalinka J, Chabowski A, and Laudanski P. 2017.
413 Sphingolipids as a new factor in the pathomechanism of preeclampsia - Mass spectrometry analysis. *PLoS*
414 *One* 12:e0177601.

415 Chen X, Li X, Guo J, Zhang P, and Zeng W. 2017. The roles of microRNAs in regulation of mammalian
416 spermatogenesis. *J Anim Sci Biotechnol* 8:35.

417 Clara JA, Monge C, Yang Y, and Takebe N. 2019. Targeting signalling pathways and the immune microenvironment
418 of cancer stem cells - a clinical update. *Nat Rev Clin Oncol*.

419 Dominissini D, Moshitch-Moshkovitz S, Schwartz S, Salmon-Divon M, Ungar L, Osenberg S, Cesarkas K, Jacob-Hirsch
420 J, Amariglio N, Kupiec M, Sorek R, and Rechavi G. 2012. Topology of the human and mouse m6A RNA
421 methylomes revealed by m6A-seq. *Nature* 485:201-206.

422 Edupuganti RR, Geiger S, Lindeboom RGH, Shi H, Hsu PJ, Lu Z, Wang SY, Baltissen MPA, Jansen P, Rossa M, Muller
423 M, Stunnenberg HG, He C, Carell T, and Vermeulen M. 2017. N(6)-methyladenosine (m(6)A) recruits and
424 repels proteins to regulate mRNA homeostasis. *Nat Struct Mol Biol* 24:870-878.

425 Fu Y, Dominissini D, Rechavi G, and He C. 2014. Gene expression regulation mediated through reversible m(6)A
426 RNA methylation. *Nat Rev Genet* 15:293-306.

427 Herzog EM, Eggink AJ, Willemsen SP, Slieker RC, Wijnands KPJ, Felix JF, Chen J, Stubbs A, van der Spek PJ, van
428 Meurs JB, and Steegers-Theunissen RPM. 2017. Early- and late-onset preeclampsia and the tissue-specific
429 epigenome of the placenta and newborn. *Placenta* 58:122-132.

430 Hiden U, Bilban M, Knofler M, and Desoye G. 2007. Kisspeptins and the placenta: regulation of trophoblast

invasion. *Rev Endocr Metab Disord* 8:31-39.

Huang H, Weng H, Sun W, Qin X, Shi H, Wu H, Zhao BS, Mesquita A, Liu C, Yuan CL, Hu YC, Huttelmaier S, Skibbe JR, Su R, Deng X, Dong L, Sun M, Li C, Nachtergaele S, Wang Y, Hu C, Ferchen K, Greis KD, Jiang X, Wei M, Qu L, Guan JL, He C, Yang J, and Chen J. 2018. Recognition of RNA N(6)-methyladenosine by IGF2BP proteins enhances mRNA stability and translation. *Nat Cell Biol* 20:285-295. 10.1038/s41556-018-0045-z

Junus K, Centlow M, Wikstrom AK, Larsson I, Hansson SR, and Olovsson M. 2012. Gene expression profiling of placentae from women with early- and late-onset pre-eclampsia: down-regulation of the angiogenesis-related genes ACVRL1 and EGFL7 in early-onset disease. *Mol Hum Reprod* 18:146-155.

Krishnamurthy N, and Kurzrock R. 2018. Targeting the Wnt/beta-catenin pathway in cancer: Update on effectors and inhibitors. *Cancer Treat Rev* 62:50-60.

Liang M, Niu J, Zhang L, Deng H, Ma J, Zhou W, Duan D, Zhou Y, Xu H, and Chen L. 2016. Gene expression profiling reveals different molecular patterns in G-protein coupled receptor signaling pathways between early- and late-onset preeclampsia. *Placenta* 40:52-59.

Liu N, Zhou KI, Parisien M, Dai Q, Diatchenko L, and Pan T. 2017a. N6-methyladenosine alters RNA structure to regulate binding of a low-complexity protein. *Nucleic Acids Res* 45:6051-6063.

Liu X, Chen H, Kong W, Zhang Y, Cao L, Gao L, and Zhou R. 2017b. Down-regulated long non-coding RNA-ATB in preeclampsia and its effect on suppressing migration, proliferation, and tube formation of trophoblast cells. *Placenta* 49:80-87.

Ma JZ, Yang F, Zhou CC, Liu F, Yuan JH, Wang F, Wang TT, Xu QG, Zhou WP, and Sun SH. 2017. METTL14 suppresses the metastatic potential of hepatocellular carcinoma by modulating N(6) -methyladenosine-dependent primary MicroRNA processing. *Hepatology* 65:529-543.

Magee LA, Pels A, Helewa M, Rey E, and von Dadelszen P. 2014. Diagnosis, evaluation, and management of the hypertensive disorders of pregnancy: executive summary. *J Obstet Gynaecol Can* 36:416-441.

Meyer KD, and Jaffrey SR. 2014. The dynamic epitranscriptome: N6-methyladenosine and gene expression control. *Nat Rev Mol Cell Biol* 15:313-326.

Mol BWJ, Roberts CT, Thangaratinam S, Magee LA, de Groot CJM, and Hofmeyr GJ. 2016. Pre-eclampsia. *Lancet* 387:999-1011.

Molvarec A, Szarka A, Walentin S, Beko G, Karadi I, Prohaszka Z, and Rigo J, Jr. 2011. Serum heat shock protein 70 levels in relation to circulating cytokines, chemokines, adhesion molecules and angiogenic factors in women with preeclampsia. *Clin Chim Acta* 412:1957-1962.

Muller-Deile J, Schroder P, Beverly-Staggs L, Hiss R, Fiedler J, Nystrom J, Thum T, Haller H, and Schiffer M. 2018. Overexpression of preeclampsia induced microRNA-26a-5p leads to proteinuria in zebrafish. *Sci Rep* 8:3621.

Myatt L, and Webster RP. 2009. Vascular biology of preeclampsia. *J Thromb Haemost* 7:375-384.

Nikuei P, Rajaei M, Malekzadeh K, Nejatizadeh A, Mohseni F, Poordarvishi F, Ghashghaeezadeh N, and Mohtarami M. 2017. Expression of placental growth factor mRNA in preeclampsia. *Int J Reprod Biomed (Yazd)* 15:169-174.

Novakovic B, and Saffery R. 2012. The ever growing complexity of placental epigenetics - role in adverse pregnancy outcomes and fetal programming. *Placenta* 33:959-970.

Nusse R, and Clevers H. 2017. Wnt/beta-Catenin Signaling, Disease, and Emerging Therapeutic Modalities. *Cell* 169:985-999.

Padmanabhan N, Jia D, Geary-Joo C, Wu X, Ferguson-Smith AC, Fung E, Bieda MC, Snyder FF, Gravel RA, Cross JC, and Watson ED. 2013. Mutation in folate metabolism causes epigenetic instability and transgenerational effects on development. *Cell* 155:81-93.

Pereira AC, Paulo M, Araujo AV, Rodrigues GJ, and Bendhack LM. 2011. Nitric oxide synthesis and biological functions of nitric oxide released from ruthenium compounds. *Braz J Med Biol Res* 44:947-957.

Piao M, Sun L, and Zhang QC. 2017. RNA Regulations and Functions Decoded by Transcriptome-wide RNA Structure Probing. *Genomics Proteomics Bioinformatics* 15:267-278.

Redman CW, Sargent IL, and Staff AC. 2014. IFPA Senior Award Lecture: making sense of pre-eclampsia - two placental causes of preeclampsia? *Placenta* 35 Suppl:S20-25.

Salomon C, Scholz-Romero K, Sarker S, Sweeney E, Kobayashi M, Correa P, Longo S, Duncombe G, Mitchell MD, Rice GE, and Illanes SE. 2016. Gestational Diabetes Mellitus Is Associated With Changes in the Concentration and Bioactivity of Placenta-Derived Exosomes in Maternal Circulation Across Gestation. *Diabetes* 65:598-609.

Sheikhi A, Razdar S, Rahmanpour H, Mousavinasab N, Ganji HB, and Jafarzadeh A. 2015. Higher expression of HSP70 and LOX-1 in the placental tissues of pre-eclampsia pregnancies. *Clin Exp Hypertens* 37:128-135.

Shi H, Wang X, Lu Z, Zhao BS, Ma H, Hsu PJ, Liu C, and He C. 2017. YTHDF3 facilitates translation and decay of N(6)-methyladenosine-modified RNA. *Cell Res* 27:315-328.

Sitras V, Paulssen RH, Gronaas H, Leirvik J, Hanssen TA, Vartun A, and Acharya G. 2009. Differential placental gene expression in severe preeclampsia. *Placenta* 30:424-433.

Taniguchi K, Kawai T, Kitawaki J, Tomikawa J, Nakabayashi K, Okamura K, Sago H, and Hata K. 2020. Epitranscriptomic profiling in human placenta: N6-methyladenosine modification at the 5'-untranslated region is related to fetal growth and preeclampsia. *FASEB J* 34:494-512. 10.1096/fj.201900619RR

Veras E, Kurman RJ, Wang TL, and Shih IM. 2017. PD-L1 Expression in Human Placentas and Gestational Trophoblastic Diseases. *Int J Gynecol Pathol* 36:146-153.

Wang T, Xiang Y, Zhou X, Zheng X, Zhang H, Zhang X, Zhang J, He L, and Zhao X. 2019. Epigenome-wide association data implicate fetal/maternal adaptations contributing to clinical outcomes in preeclampsia. *Epigenomics* 11:1003-1019.

Wang X, Lu Z, Gomez A, Hon GC, Yue Y, Han D, Fu Y, Parisien M, Dai Q, Jia G, Ren B, Pan T, and He C. 2014. N6-methyladenosine-dependent regulation of messenger RNA stability. *Nature* 505:117-120.

Wang X, Zhao BS, Roundtree IA, Lu Z, Han D, Ma H, Weng X, Chen K, Shi H, and He C. 2015. N(6)-methyladenosine Modulates Messenger RNA Translation Efficiency. *Cell* 161:1388-1399.

Wilson SL, Leavey K, Cox BJ, and Robinson WP. 2018. Mining DNA methylation alterations towards a classification of placental pathologies. *Hum Mol Genet* 27:135-146.

Witkin SS, Kanninen TT, and Sisti G. 2017. The Role of Hsp70 in the Regulation of Autophagy in Gametogenesis, Pregnancy, and Parturition. *Adv Anat Embryol Cell Biol* 222:117-127.

Wu F, Tian FJ, Lin Y, and Xu WM. 2016. Oxidative Stress: Placenta Function and Dysfunction. *Am J Reprod Immunol* 76:258-271.

Yang Y, Hsu PJ, Chen YS, and Yang YG. 2018. Dynamic transcriptomic m(6)A decoration: writers, erasers, readers and functions in RNA metabolism. *Cell Res* 28:616-624.

Yeung KR, Chiu CL, Pidsley R, Makris A, Hennessy A, and Lind JM. 2016. DNA methylation profiles in preeclampsia and healthy control placentas. *Am J Physiol Heart Circ Physiol* 310:H1295-1303.

513 Yue Y, Liu J, and He C. 2015. RNA N6-methyladenosine methylation in post-transcriptional gene expression
514 regulation. *Genes Dev* 29:1343-1355.
515 Zhang M, Muralimanoharan S, Wortman AC, and Mendelson CR. 2016. Primate-specific miR-515 family members
516 inhibit key genes in human trophoblast differentiation and are upregulated in preeclampsia. *Proc Natl*
517 *Acad Sci U S A* 113:E7069-E7076.
518 Zhang S, Zhao BS, Zhou A, Lin K, Zheng S, Lu Z, Chen Y, Sulman EP, Xie K, Bogler O, Majumder S, He C, and Huang S.
519 2017a. m(6)A Demethylase ALKBH5 Maintains Tumorigenicity of Glioblastoma Stem-like Cells by
520 Sustaining FOXM1 Expression and Cell Proliferation Program. *Cancer Cell* 31:591-606.e596.
521 Zhang Z, Wang X, Zhang L, Shi Y, Wang J, and Yan H. 2017b. Wnt/beta-catenin signaling pathway in trophoblasts
522 and abnormal activation in preeclampsia (Review). *Mol Med Rep* 16:1007-1013.
523 Zheng Q, Hou J, Zhou Y, Li Z, and Cao X. 2017. The RNA helicase DDX46 inhibits innate immunity by entrapping
524 m(6)A-demethylated antiviral transcripts in the nucleus. *Nat Immunol* 18:1094-1103.
525 Zhou J, Wan J, Gao X, Zhang X, Jaffrey SR, and Qian SB. 2015. Dynamic m(6)A mRNA methylation directs
526 translational control of heat shock response. *Nature* 526:591-594. 10.1038/nature15377

527

Table 1(on next page)

Clinical information of samples used in the study.

1 **Table 1. Clinical information of samples used in the study.**

Characteristic	Preeclampsia (n=4)	Control (n=4)	P Value
Maternal age, year	29.5 ± 1.3	29 ± 0.8	0.54
Gestational age, week	37.9 ± 0.5	38.2 ± 0.4	0.41
Prenatal maternal body mass index, kg/m2	27.6 ± 1.2	27.7 ± 0.8	0.86
Diastolic pressure, mmHg	110.3 ± 7.1	80 ± 4.2	3.40E-04
Systolic pressure, mmHg	162.5 ± 4.8	124.5 ± 4.9	3.27E-05
Proteinuria,g/24h	4.1 ± 0.5	0 ± 0	4.08E-04
Birth weight, g	3567.3 ± 290.2	3339 ± 316.6	0.33

2

3

Table 2(on next page)

Sequencesof primers used for qRT-PCR analysis of mRNA levels.

Table 2. Sequences of primers used for qRT-PCR analysis of mRNA levels.

Gene name	Primer	Sequence	Product size (bp)
METTL3	Forward	5' ACAGAGTGTCGGAGGTGATT 3'	201
	Reverse	5' TGTAGTACGGGTATGTTGAGC 3'	
METTL14	Forward	5' TGAGATTGCAGCACCTCGAT 3'	250
	Reverse	5' AATGAAGTCCCCGTCTGTGC 3'	
WTAP	Forward	5' CCTCTTCCCAAGAAGGTTCGAT 3'	238
	Reverse	5' GTTCCTTGGTTGCTAGTCGC 3'	
FTO	Forward	5' AATAGCCGCTGCTTGTGAG 3'	182
	Reverse	5' CCACTTCATCTTGTCCGTTG 3'	
ALKBH5	Forward	5' GCCGTCATCAACGACTACCA 3'	208
	Reverse	5' ATCCACTGAGCACAGTCACG 3'	
β-actin	Forward	5' GTGGCCGAGGACTTTGATTG 3'	73
	Reverse	5' CCTGTAACAACGCATCTCATATT 3'	

Table 3(on next page)

The top 20 differently expressed m6A peaks inPE.

1 **Table 3. The top 20 differently expressed m6A peaks in PE.**

Gene name	fold change	Regulation	Chromosome	Peak start	Peak end	Peak region	P-value
HSPA1A	47.50	Up	GL000251.1	3294734	3294974	cds	5.13E-06
DMWD	18.38	Up	chr19	46293970	46294029	cds, utr3	1.82E-02
HYOU1	15.67	Up	JH159138.1	67181	68226	cds, utr3	5.62E-03
BRCA1	15.14	Up	chr17	41245740	41245861	cds	6.61E-03
NDUFB2	13.36	Up	chr7	140396821	140400705	utr5	4.79E-02
SLC39A1	13.09	Up	chr1	153939949	153940038	utr5	1.38E-02
HYOU1	13.00	Up	JH159138.1	67162	68237	cds, utr3	7.94E-03
SCAF11	13.00	Up	chr12	46322790	46322910	utr5	2.75E-02
SLC25A29	12.47	Up	chr14	100760163	100760343	utr5	2.63E-02
MID1IP1	9.99	Up	chrX	38663134	38663344	utr5	1.55E-02
SLC6A2	0.07	Down	chr16	55689515	55689784	utr5	1.41E-02
NPIPB6	0.08	Down	chr16	28353905	28354053	utr3, cds	7.59E-03
LEKR1	0.09	Down	chr3	156544207	156544506	utr5	1.38E-02
MBLAC2	0.09	Down	chr5	89769658	89769897	cds	2.19E-02
TSSK6	0.10	Down	chr19	19626179	19626300	cds, utr5	3.16E-02
LRRC3	0.10	Down	chr21	45877072	45877311	cds, utr3	3.47E-02
RSPO1	0.12	Down	chr1	38077963	38078322	utr3	4.90E-02
AC016586.1	0.13	Down	chr19	4041364	4041783	utr3	6.17E-03
TEX40	0.14	Down	chr11	64071267	64072238	cds, utr3	3.16E-02
RPP25	0.15	Down	chr15	75246876	75246966	utr3	4.90E-02

2

3

Table 4(on next page)

The top 20 differently expressed genes in PE.

Table 4. The top 20 differently expressed genes in PE.

Gene name	Fold change	Regulation	Locus	Strand	p_value
AOC1	8.51	Up	chr7:150521715-150558592	+	5.48E-04
HLA-DRB5	4.45	Up	chr6:32485120-32498064	-	4.50E-02
DIO2	4.31	Up	chr14:80663870-80854100	-	4.09E-03
NOTUM	4.27	Up	chr17:79910383-79919716	-	3.34E-02
SPIN1	4.04	Up	chr9:91003334-91093609	+	1.26E-03
LAIR2	3.55	Up	chr19:55009100-55021897	+	3.46E-03
PLAC8	2.96	Up	chr4:84011201-84058228	-	2.89E-02
DCD	2.61	Up	chr12:55038375-55042277	-	4.97E-02
UPK1B	2.57	Up	chr3:118892364-118924000	+	2.42E-02
PTPRCAP	2.57	Up	chr11:67202981-67205538	-	3.48E-03
H2AFJ	0.67	Down	chr12:14927317-14930936	+	2.06E-02
AHSA2	0.67	Down	chr2:61404553-61418338	+	2.87E-02
B3GNT2	0.66	Down	chr2:62423248-62451866	+	2.51E-02
PAK1	0.66	Down	chr11:77032752-77185680	-	4.96E-02
TMEM14B	0.66	Down	chr6:10747992-10852986	+	8.71E-03
IMPA2	0.66	Down	chr18:11981024-12030882	+	2.68E-04
PKNOX2	0.65	Down	chr11:125034583-125303285	+	3.23E-04
SLC9A6	0.65	Down	chrX:135056000-135129428	+	1.21E-02
HIST4H4	0.63	Down	chr12:14920933-14924065	-	1.74E-02
ANKRD33	0.63	Down	chr12:52281744-52285448	+	1.61E-02

Figure 1

METTL3and METTL14 were up-regulated in PE.

Quantitative real-time PCR was used to analysis the mRNA levels of METTL3, METTL14, FTO, WTAP, and ALKBH5 in the PE samples and samples from normal pregnant women. All p-values were calculated using Student's t-test. *$p < 0.05$ versus control group ($n = 4$ each). PE: preeclampsia.

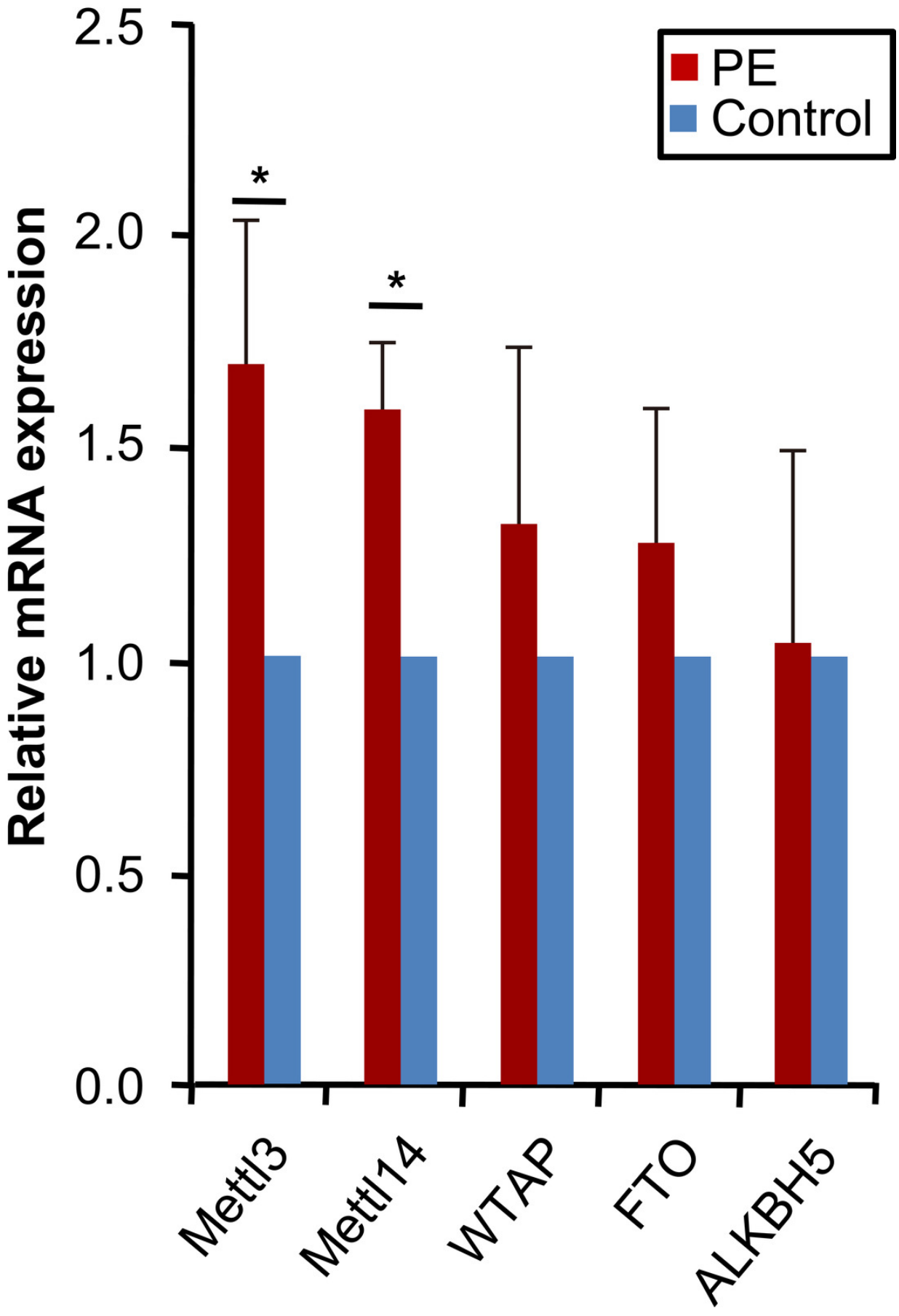
PE
Control
Relative mRNA expression
2.5
2.0
1.5
1.0
0.5
0.0
*
*
Mettl3
Mettl14
WTAP
FTO
ALKBH5

Figure 2

M6Alevels of total RNA in PE and control.

M6A levels of total RNA were determined by antibody based colorimetric method. Data are presented as mean ± SD. All p-values were calculated using Student's t-test. **p < 0.01 versus control group (n = 4 each). PE: preeclampsia.

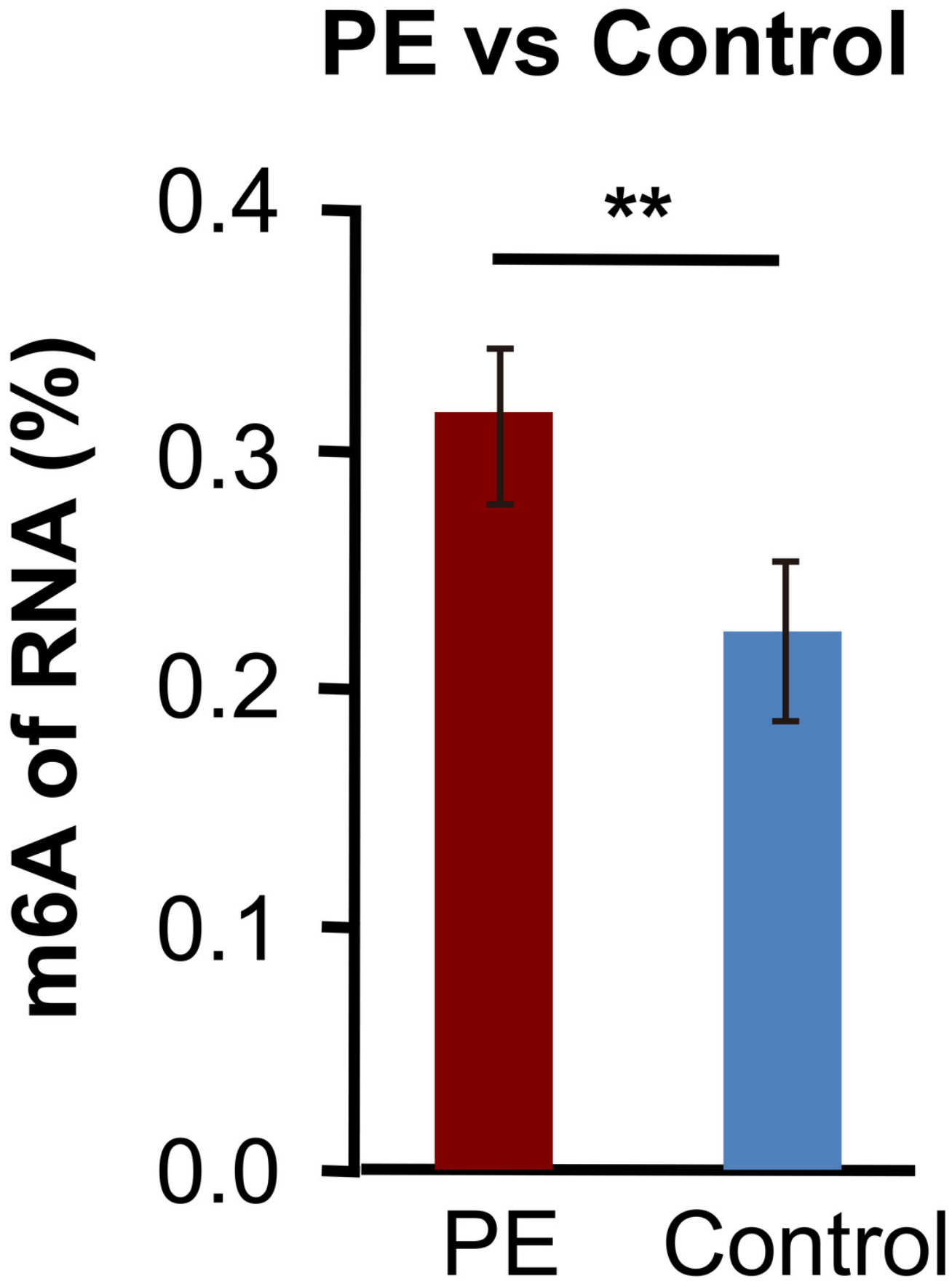
PE vs Control
**
m6A of RNA (%)
0.4
0.3
0.2
0.1
0.0
PE
Control

Figure 3

Overviewof the m6A methylation landscape in the preeclampsia and control samples.

The M6A-tagged transcript map was profiled using m6A-RIP-seq. (A) Volcano plots displaying the distinct m6A peaks and their statistical significance (fold changes ≥1.5 and $p < 0.05$). (B) Metagene plots showing the region of average m6A peaks throughout the transcripts in the preeclampsia and control samples. (C) Pie charts displaying the distribution of m6A peaks in the preeclampsia. (D) Pie charts displaying the distribution of m6A peaks in the control group. (E) Distributions of altered m6A peaks in human chromosomes. (F) Sequence motifs of the m6A-containing peak regions. (G) Data visualisation analysis of *HSPA1A* mRNA m6A modifications in the preeclampsia group. (H) Data visualisation analysis of *HSPA1A* mRNA m6A modifications in the control group. m6A-RIP-seq: m6A RNA immunoprecipitation sequencing.

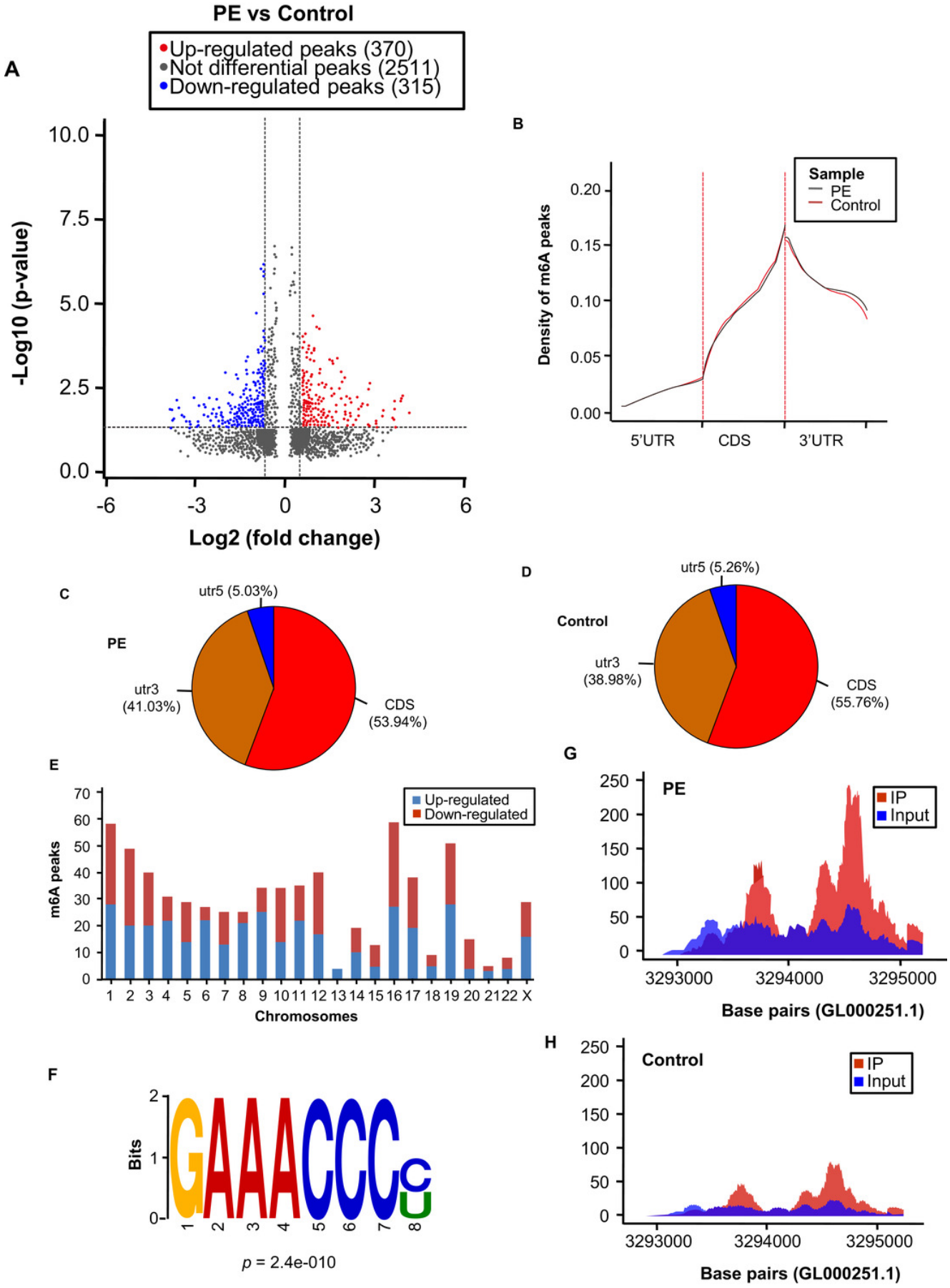
A
PE vs Control
Up-regulated peaks (370)
Not differential peaks (2511)
Down-regulated peaks (315)
-Log10 (p-value)
Log2 (fold change)
B
Sample
PE
Control
Density of m6A peaks
5'UTR
CDS
3'UTR
C
PE
utr5 (5.03%)
utr3 (41.03%)
CDS (53.94%)
D
Control
utr5 (5.26%)
utr3 (38.98%)
CDS (55.76%)
E
Up-regulated
Down-regulated
m6A peaks
Chromosomes
F
Bits
p = 2.4e-010
G
PE
IP
Input
Base pairs (GL000251.1)
H
Control
IP
Input
Base pairs (GL000251.1)

Figure 4(on next page)

Overviewof the m6A methylation landscape in the preeclampsia and control samples. Geneontology and KEGG pathway analyses of the altered m6A transcripts.

(A) Major enriched and significant GO-assessed up-regulated m6A peak transcripts. (B) Major enriched and significant GO-assessed down-regulated m6A peaks transcripts. (C) The top ten significantly enriched pathways for the up-regulated m6A peaks transcripts. (D) The top ten significantly enriched pathways for the down-regulated m6A peaks transcripts. GO: gene ontology, KEGG: Kyoto encyclopedia of genes and genomes, BP: biological process, CC: cellular component, MF: molecular function.

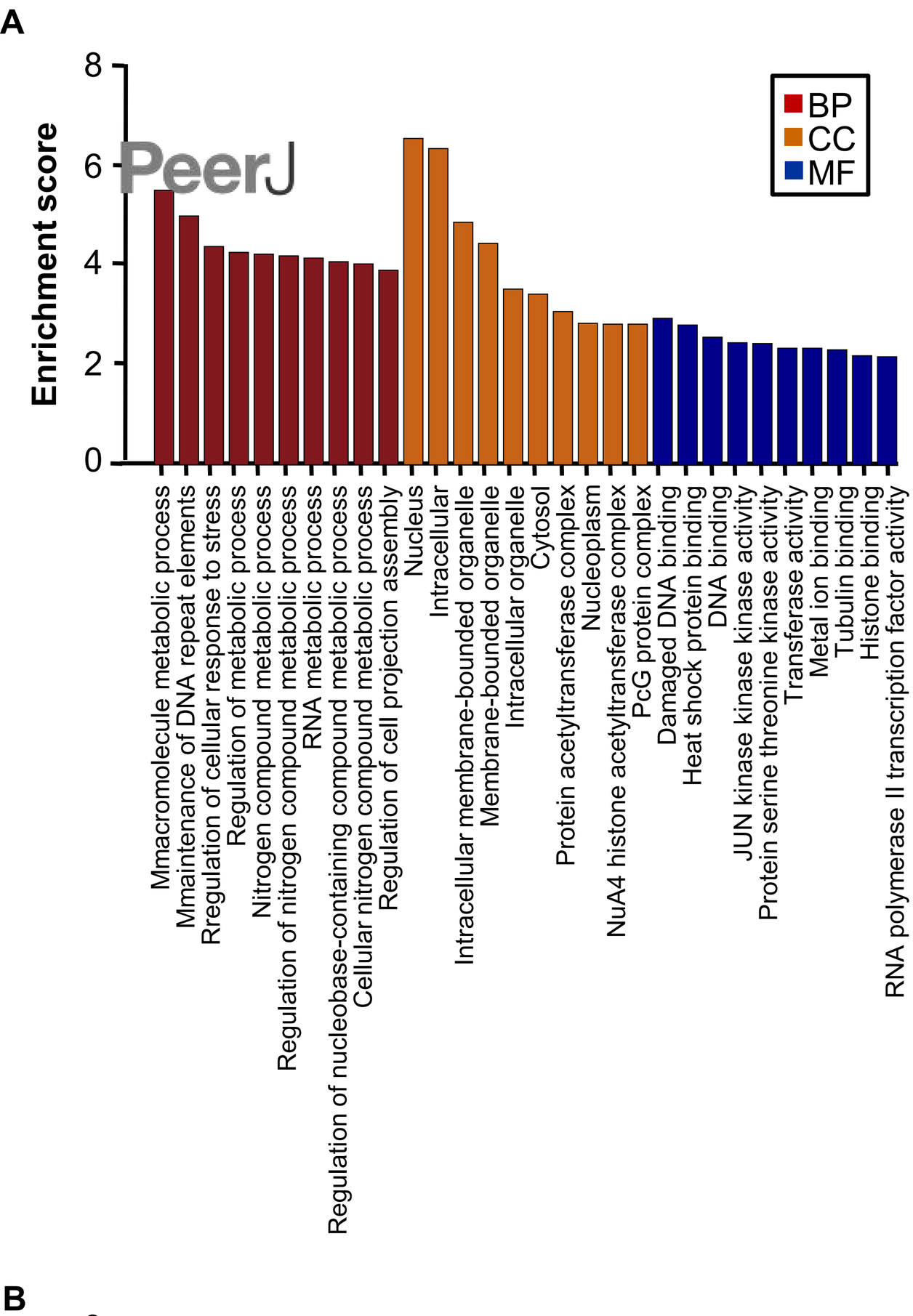

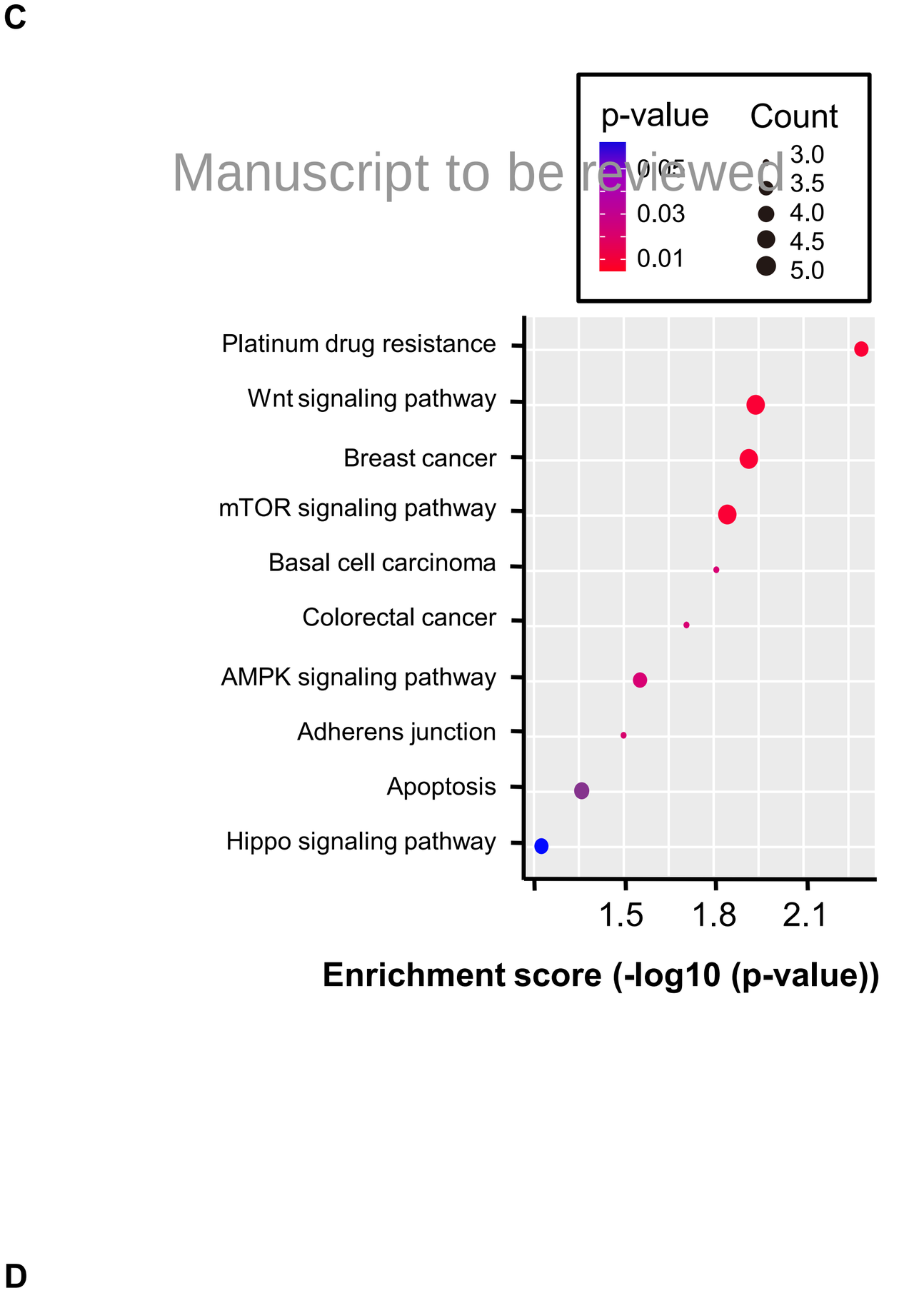

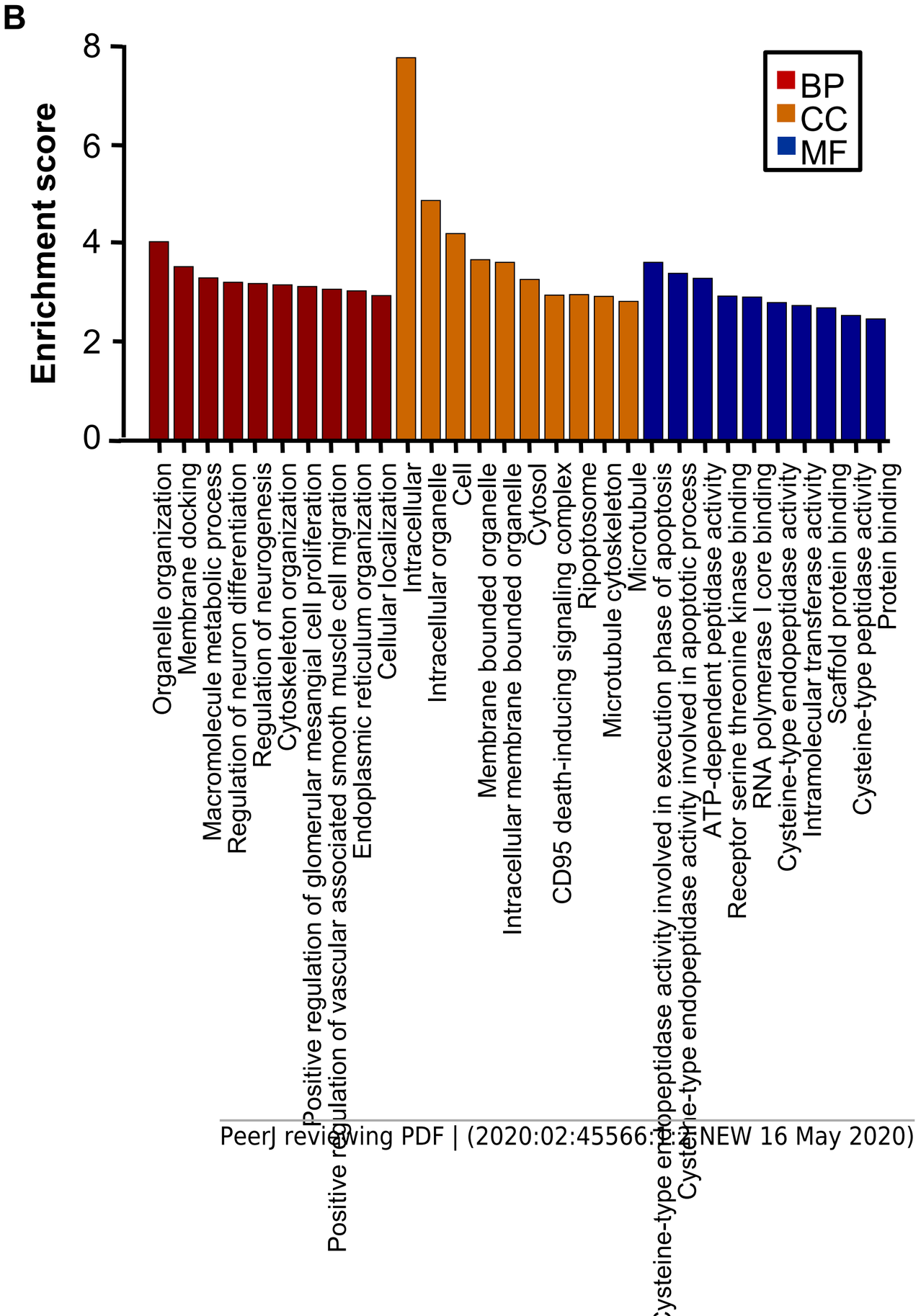

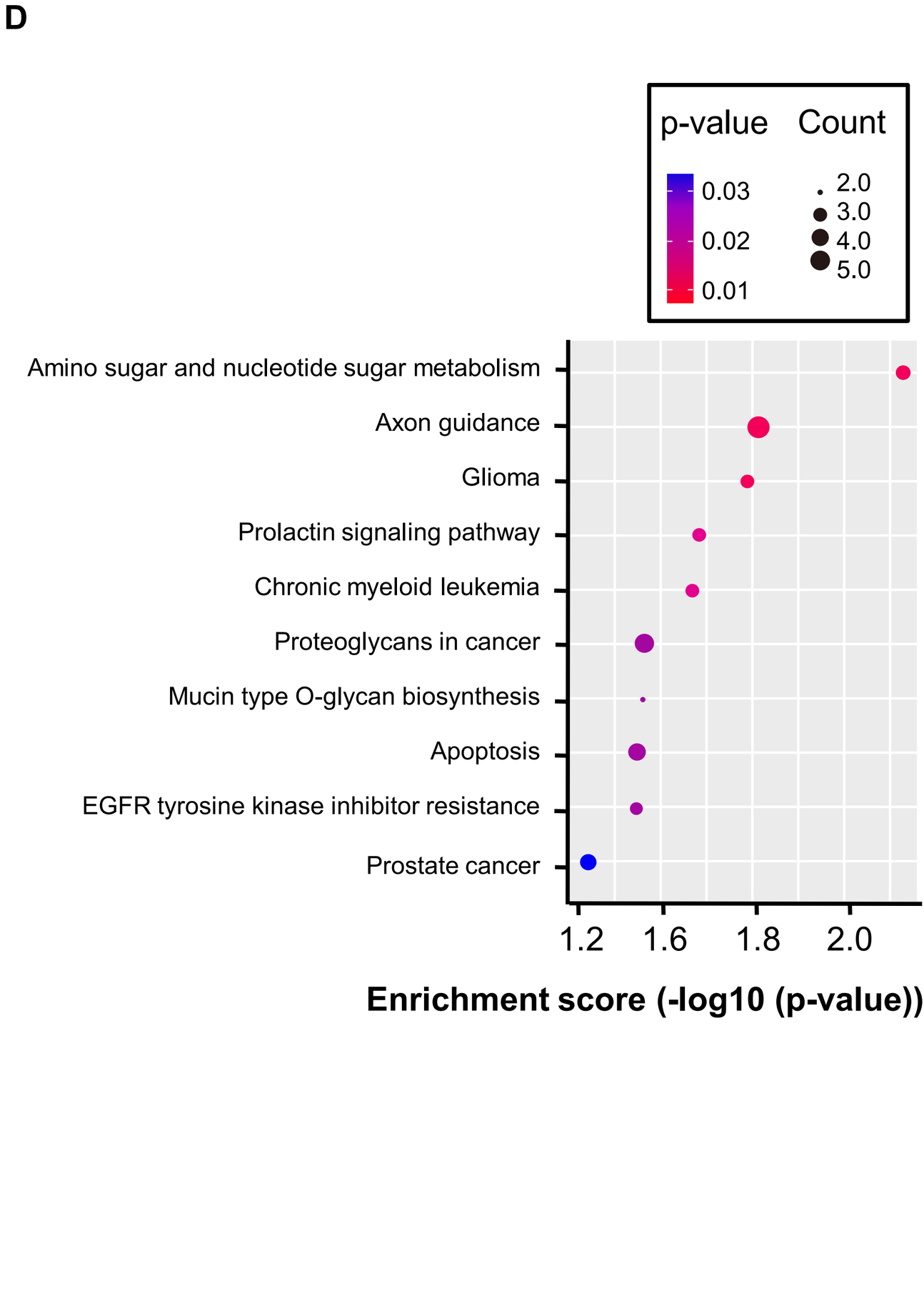

Figure 5

Conjointanalysis of m6A-RIP-seq and RNA-sequencing data for preeclampsia and controlsamples.

(A) Volcano plots displaying the mRNAs that were differentially expressed between the preeclampsia and control groups and their statistical significance (fold changes ≥1.5 and $p < 0.05$). (B) Hierarchical clustering analysis of the differentially expressed mRNAs. (C) Three-dimensional plot reveals the predicted novel transcripts as assessed by the coding potential assessing tool. (D) Four quadrant graph showing the distribution of transcripts with a significant change in both m6A level and expression in preeclampsia.

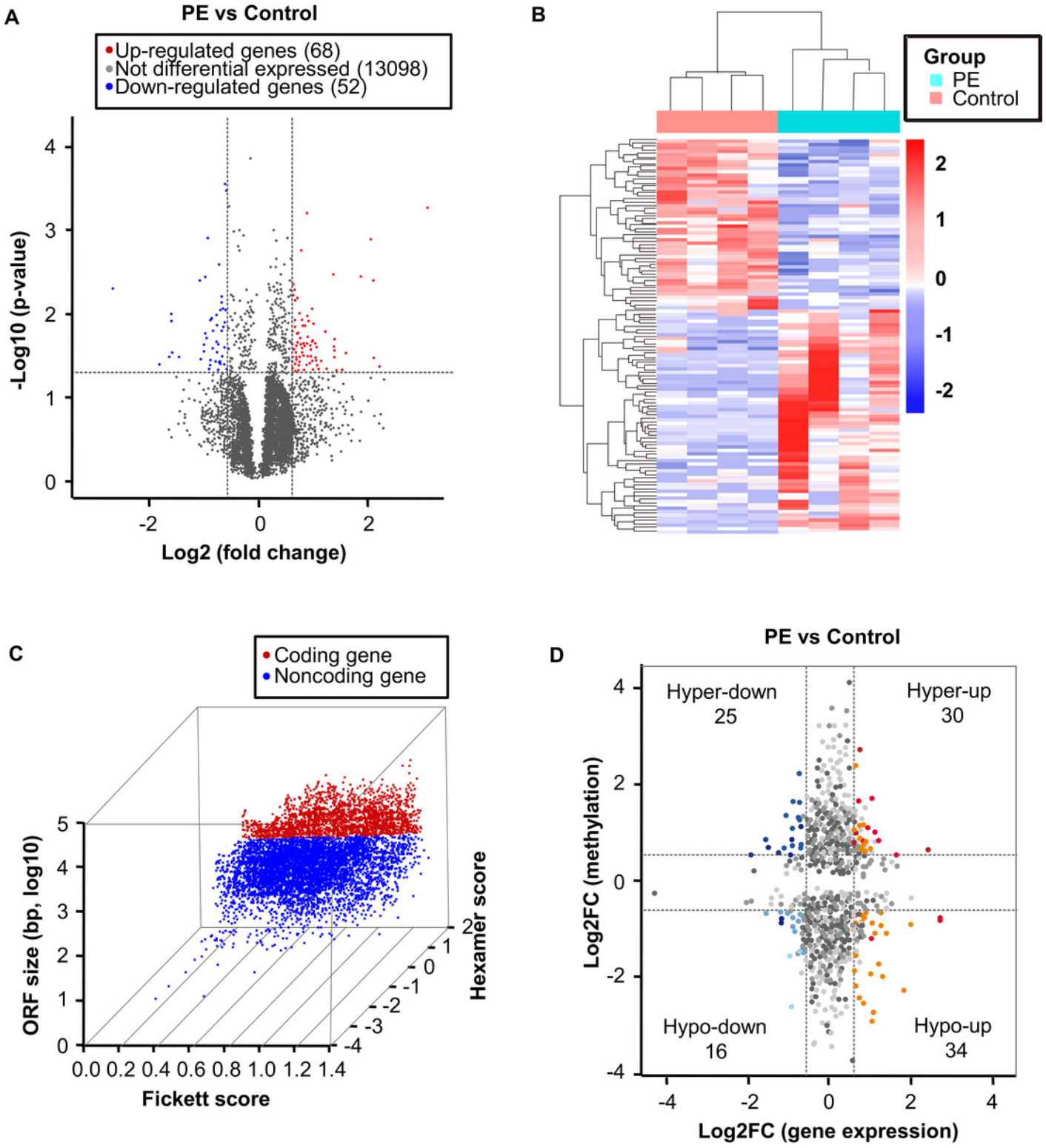
A
PE vs Control
Up-regulated genes (68)
Not differential expressed (13098)
Down-regulated genes (52)
-Log10 (p-value)
Log2 (fold change)
B
Group
PE
Control
2
1
0
-1
-2
C
Coding gene
Noncoding gene
ORF size (bp, log10)
Fickett score
Hexamer score
D
PE vs Control
Hyper-down
25
Hyper-up
30
Hypo-down
16
Hypo-up
34
Log2FC (methylation)
Log2FC (gene expression)